Tikrit Journal of Pure Science Vol. 30 (6) 2025

DOI: https://doi.org/10.25130/tjps.v30i6.1787

IRAQI Academic Scientific Journals

Tikrit Journal of Pure Science

ISSN: 1813 – 1662 (Print) --- E-ISSN: 2415 – 1726 (Online)

Journal Homepage: https://tjpsj.org/

Tikrit Journal of Pure Science

Optimization of Tin-Based Lead-Free Perovskite Solar Cells Using SCAPS-1D: Investigating ETL and HTL Materials for Enhanced Efficiency

Chnar I. Hussain[1], **Yousif M. Hassan**[1], **Farah A. Abed**[2]

[1] *Physics Department, College of Science/ Salahaddin University, Erbil – Iraq*

[2]*Industrial Automation Technology Department, Erbil Technology College/ Erbil Polytechnic University, Iraq*

Received: 7 Oct. 2024 **Received in revised forum:** 10 Feb. 2025 **Accepted:** 18 Feb. 2025

Final Proof Reading: 25 Mar. 2025 **Available online:** 25 Dec. 2025

ABSTRACT

The Solar Cell Capacitance Simulator (SCAPS-1D) software is used to investigate the optimal use of methylammonium tin chloride as the active material in perovskite solar cells (PSCs), a new class of solar cells. The formulation of PSC is as follows: FTO/ETL/$CH_3NH_3SnCl_3$/HTL/Au. To improve the performance of perovskite solar cells, various materials, such as IGZO, SnO2, TiO2, and ZnO, are tested as electron transport layers (ETLs), and Spiro-OMeTAD, NiO, Cu2O, and CuO are tested as hole transport layers (HTLs). The study shows that among these ETLs, SnO_2 records the highest potential to achieve high energy conversion (η) when combined with Spiro-OMeTAD as the HTLs. In addition, the total defects (N_t) were studied in the PSC by keeping N_t constant in the first two layers and varying N_t in the third layer. The results show that PSC is indeed efficient; It is desirable to have a N_t of (10^{15} cm^{-3}) for the ETL (SnO_2), (10^9 cm^{-3}) for the absorber layer ($CH_3NH_3SnCl_3$), and (10^{14} cm^{-3}) for the HTL (SpiroOMeTAD). The power conversion efficiency has increased for this output value to (13.68 %) with an open circuit voltage (V_{oc}) of (1.6 V). This development aims to enhance the performance of environmentally friendly, lead-free solar cells based on tin-based perovskite materials.

Keywords: SCAPS-1D, ETL, HTL, Total defects density

Name: **Chnar I. Hussain** **E-mail:** chnar.hussain@su.edu.krd

Tikrit Journal of Pure Science Vol. 30 (6) 2025
DOI: https://doi.org/10.25130/tjps.v30i6.1787

تحسين الخلايا الشمسية المصنوعة من البيروفسكايت الخالية من الرصاص والمعتمدة على القصدير باستخدام SCAPS-1D: دراسة مواد ETL وHTL لتحسين الكفاءة

جنار إبراهيم حسين[1]، يوسف مولود حسن[1]، فرح عامر عابد[2]

[1] قسم الفيزياء، كلية العلوم، جامعة صلاح الدين، أربيل، العراق

[2] قسم تكنولوجيا الأتمتة الصناعية، كلية أربيل للتكنولوجيا، جامعة أربيل التقنية، أربيل، العراق

الملخص

تم استخدام برنامج محاكاة سعة الخلية الشمسية (SCAPS-1D) في هذه الدراسة لإيجاد أفضل طريقة لاستخدام كلوريد ميثيل أمونيوم القصدير كمكون نشط في خلية شمسية بيروفسكايت (PSC)، وهي نوع جديد من الخلايا الشمسية. تم بإعداد بنية PSC على النحو التالي: FTO/ETL/$CH_3NH_3SnCl_3$/HTL/Au. لتحسين أداء الخلايا الشمسية بيروفسكايت، تم باختبار مواد مختلفة، مثل IGZO وSnO_2 وTiO_2 و ZnO كطبقات نقل الإلكترون (ETLs) و Spiro-OMeTAD و NiO و Cu_2O و CuO كطبقات نقل الثقوب (HTLs). تشير النتائج إلى أنه من بين هذه الطبقات، يُظهر SnO_2 أعلى إمكانية لتحقيق كفاءة (η) تحويل عالية للطاقة عند دمج مع Spiro-OMeTAD كطبقة نقل الثقوب. علاوة على ذلك، تم دراسة كثافة العيوب الكلية (N_t) في خلية وذلك بالحفاظ على N_t للطبقتين الأوليين ثابتة وتغيير N_t في الطبقة الثالثة. تظهر نتائج أن خلية تعمل بشكل جيد. تبين أن يكون N_t لـ (SnO_2 ETL) تساوي (10^{15} cm^{-3}) و(10^{9} cm^{-3}) لطبقة ($CH_3NH_3SnCl_3$) الماصة و(10^{14} cm^{-3}) لـ (HTL SpiroOMeTAD). بذلك تم الحصول على كفاءة تحويل الطاقة (13.68 %) وفولتية دائرة مفتوحة (V_{oc}) تساوي (1.6 V). من المتوقع أن يعزز هذا التقدم أداء الخلايا الشمسية الصديقة للبيئة والخالية من الرصاص والتي تستخدم مواد البيروفسكايت القائمة على القصدير.

INTRODUCTION

Perovskite solar cells are a breakthrough in renewable energy research that addresses the limitations of silicon solar cells. Its superior performance has the potential to benefit humanity (1,2) greatly. The inclusion of lead (Pb) in PSCs can have adverse environmental effects, making it undesirable for society. The non-poisonous detail tin (Sn) is placed in the same institution as lead (Pb) on the periodic desk [(3)]. It would be interesting to examine the consequences of replacing Pb by Sn in $CH_3NH_3PbX_3$. To achieve efficient solar-cell performance, lead-free natural PSCs must possess the same optical, structural, and photovoltaic properties as their lead counterparts [(4)]. The replacement of Pb by Sn in the open field for the fabrication of $CH_3NH_3SnCl_3$ photoelectric cells in the presence of high chlorine (Cl) and excess Cl has a positive effect on system improvement of the film [(3,5)]. In addition, it prevents the oxidation of Sn in atmospheric oxygen, thereby maintaining the same chemical state as the raw materials [(3,5-7)]. In this regard, $CH_3NH_3SnCl_3$ has been used as an adsorbent to reduce the toxicity (4). The direct band gap of these materials ranges from (2.15 to 3.59 eV) [(3,8)]. Consequently, it is believed that these solar cells, which are based on perovskite, will exhibit a substantial short-circuit current. Several challenging elements must be addressed to improve the performance of Sn-based devices [(9)]. In their 2018 study, they demonstrated that the created perovskite solar cell, which utilized a solid polymer electrolyte based on polyethylene oxide, exhibited a consistent η of (0.17 %) for powdered perovskite and ultimately achieved (0.55 %) for crystalline

perovskite of $CH_3NH_3SnCl_3$ under one sun condition (100 mW/cm^2) in ambient air [10]. In addition, employed SCAPS-1D to model a lead-free device with an absorber layer composed of $CH_3NH_3SnCl_3$ (9). They aimed to optimize the device by manipulating variables such as temperature, acceptor density, thickness, and total defect density. Based on thermal stability analysis, Cl halide-based perovskites exhibit higher thermal stability. Nevertheless, the power conversion efficiency reached a value of (10.52 %). This work aims to select the best ETL and HTL layers and find the effect of total defect density of various layers on the electrical output of the perovskite solar cell and record the maximum power conversion efficiency.

ANALYTICAL METHODS

SCAPS 1D 3.3.09 is a software tool designed to model the functioning of photovoltaic cells in a one dimension. It is specifically created to simulate perovskite solar cells [11,12]. These solar cells have a glass base with a fluorine-doped tin oxide (FTO) coating that supports their standard n-i-p structure. Figure 1 illustrates the process of fabricating the different cell components, using layers of FTO as the front contact and gold (Au) as the back contact. The cell design features a layer of perovskite material ($CH_3NH_3SnCl_3$) that acts as a barrier between the ETLs and HTLs [13,14]. The common solar spectrum (AM1.5G) is used to generate the incident power density (1000 W/m^2) at (300 K).

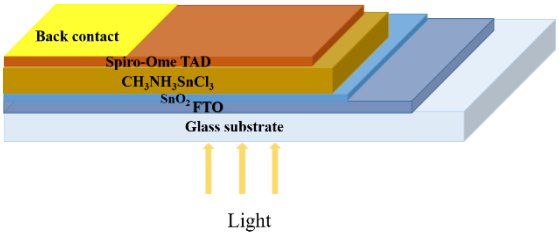

Fig. 1: Cell structure of this study: FTO/ SnO_2/ $CH_3NH_3SnCl_3$/Spiro OMe-TAD/Au

The researchers use SCAPS-1D to accurately determine the electrical properties under various lighting conditions and temperatures, as mentioned by [15]. Additionally, the SCAPS-1D program employs advanced methods based on three key equations: Poisson's equation (1), the electron transport equation (2), and the hole transport equation (3).

$$\frac{d}{dx}\left(-\varepsilon(x)\frac{d\psi}{dx}\right) = q[p(x) - n(x) + N^+ - N^- + p_t(x) - n_t(x) \quad \ldots.(1)$$

$$\frac{dp_n}{dt} = G_{p-} \frac{p_n - p_{no}}{\tau_p} - p_n \mu_p \frac{dE}{dx} - \mu_p E \frac{dp_n}{dx} + D_p \frac{d^2 p_n}{dx^2} \quad \ldots.(2)$$

$$\frac{dn_p}{dt} = G_{n-} \frac{n_p - n_{po}}{\tau_n} + n_n \mu_n \frac{dE}{dx} + \mu_n E \frac{dn_p}{dx} + D_n \frac{d^2 n_p}{dx^2} \quad \ldots. (3)$$

Where D represents the diffusion coefficient, n, p, nt, and pt stand for free electrons, free holes, trapped electrons, and trapped holes, respectively. On the other hand, G is the generation rate, τ_p is the hole lifetime, τn is the electron lifetime, μp is the electron mobility, μn is the hole mobility, q is the electron charge, E is the electric field, Ψ is the electrostatic potential, and ε is the dielectric constant. N^+ represents the ionizing acceptor- like doping concentration, while N^- represents the ionizing donor-like doping concentration, and X represents the thickness of the cell[16]. SCAPS-1D simulates PSCs using four layers, with n-type (IGZO, SnO_2, TiO_2, and ZnO) materials used to evaluate the effectiveness of each layer as an ETM. The perovskite layer (i-layer) serves as the absorber layer. Additionally, p-type materials (Spiro-OMeTAD, NiO, Cu2O, and CuO) are used individually as HTMs. Table 1 presents the material characteristics for each layer as reported in publications [16-29]. The total defect density optimization technique is utilized to detect and maintain the Nt of the previous two layers and adjust

the N_t of the third layer. Firstly, the N_t of ETL was altered from (10^{13} cm^{-3}) to (10^{20} cm^{-3}), and the total defect density of the two other layers (perovskite (10^{13} cm^{-3}) and HTL (10^{14} cm^{-3})) remained fixed. In the second phase, the total defect density of perovskite ranged from (10^{9} cm^{-3}) to ($10^{13}cm^{-3}$) while the total defect density of the two other layers (ETL (10^{14} cm^{-3}) and HTL (10^{14} cm^{-3})) remained constant. Furthermore, according to the most effective, the total defect density of HTL were observed, ranging from (10^{10} cm^{-3}) to (10^{19} cm^{-3}) while the total number of defects in the other two layers (ETL (10^{14} cm^{-3}) and perovskite (10^{7} cm^{-3})) remained stable. Finally, using the model results, the ETL (1015 cm-3), the absorbing layer (109 cm-3), and the HTL (1014 cm-3) were kept at their original total defect densities.

Table 1: Input parameters for the proposed ETL, perovskite, and HTL materials

Parameters	FTO	IGZO	SnO_2	TiO_2	ZnO	$CH_3NH_3SnCl_3$	Spiro-OMeTAD	NiO	Cu_2O	CuO
Thickness(nm)	400	35	35	35	35	900	350	350	350	350
E_g (eV)	3.5	3.05	3.6	3.2	3.3	2.15	3.17	3.8	2.17	1.48
χ (eV)	4	4.16	4	4.1	4	3.71	2.05	2.1	3	4.07
ε_r	9	10	9	9	9	3.5	3	10.7	7.1	18.1
N_c (cm^{-3})	2.2×10^{18}	5×10^{18}	2.2×10^{17}	2.2×10^{18}	2.2×10^{18}	1×10^{18}	2×10^{20}	2×10^{19}	2×10^{17}	2.1×10^{19}
N_v (cm^{-3})	1.8×10^{18}	5×10^{18}	$2.2X10^{16}$	1.8×10^{19}	1.9×10^{19}	1×10^{19}	2×10^{20}	1×10^{19}	1.1×10^{19}	5.5×10^{19}
μ_n (cm/Vs)	20	15	20	5×10^{-2}	100	1.6	2.1×10^{-3}	12	200	100
e^- thermal-velocity ($cm.s^{-1}$)	1×10^{7}	1×10^{7}	1×10^{7}	1×10^{7}	1×10^{7}	1×10^{6}	1×10^{7}	1×10^{7}	1×10^{7}	1×10^{7}
h^+ thermal-velocity ($cm.s^{-1}$)	1×10^{7}	1×10^{7}	1×10^{7}	1×10^{7}	1×10^{7}	1×10^{6}	1×10^{7}	1×10^{7}	1×10^{7}	1×10^{7}
μ_p (cm/Vs)	10	0.1	10	5×10^{-2}	25	1.6	2.16×10^{-3}	2	80	0.1
N_d (cm^{-3})	1×10^{19}	1×10^{17}	1×10^{17}	1×10^{19}	1×10^{18}	3.2×10^{18}	0	0	0	0
N_a (cm^{-3})	0	0.0	0.0	0	0	0	2×10^{19}	1.6×10^{14}	1×10^{18}	1×10^{16}
N_t (cm^{-3})	1×10^{14}	1×10^{15}	1×10^{15}	1×10^{15}	1×10^{15}	1×10^{13}	1×10^{14}	1×10^{14}	1×10^{14}	1×10^{14}

RESULTS AND DISCUSSION

Simulation of different inorganic metals ETLs:

Perovskite and Spiro-OMeTAD were used independently, with thicknesses of 900 nm and 350 nm, respectively. Table 2 reports the results of the numerical simulations. It is clear the cell-based SnO_2 layer, as compared to others, has the highest short circuit current density (J_{sc}) and η, which is (7.28 mA/cm^2) and (10.19 %), respectively. In contrast, the fill factor (FF) of the cell-based SnO2 layer (88%) was slightly higher than that of the cell-based TiO2 layer (87.67%). Furthermore, the V_{oc} of SnO2-based cell (1.58 V) is slightly increased than that of cell-based IGZO (1.53 V), TiO_2 (1.57 V), and ZnO (1.58 V). That is because the band gap energy of SnO_2 is larger than that of ZnO (3.5 eV vs. 3.3 eV) [20,30,31].

Table 2: Effects of ETLs on the output parameters of the n–i–p PSC

Cell parameters	TiO_2	SnO_2	ZnO	IGZO
V_{oc} (V)	1.57	1.58	1.58	1.53
J_{sc} (mA/cm^2)	4.79	7.28	7.10	2.33
FF (%)	87.67	88.00	87.96	87.27
η (%)	6.60	10.19	9.92	3.12

The illuminated J-V features of cell-based (IGZO, SnO_2, TiO_2, and ZnO) with a (35 nm) thickness are shown in Figure 2a. The SnO_2 layer is more transparent than the IGZO, TiO_2, and ZnO layers, thereby facilitating light absorption by the perovskite layer. [32]. This indicates that SnO2-based cells exhibit slightly better cell parameters than those based on their layers. Furthermore, both SnO_2 and ZnO exhibit substantial efficiency improvements, with values of 10.19% and 9.92%, respectively. The increased quantum efficiency (QE) of SnO_2 is based on the cell, attributed to the quantum size effect (Figure 2b).

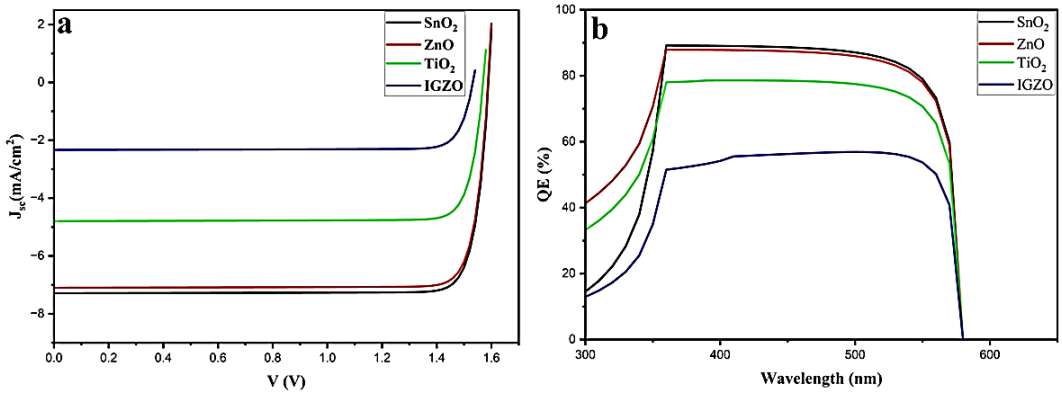

Fig. 2: (a) illuminated J-V and (b) different QE of different configuration of various ETL of the same thicknesses using Spiro-OMeTAD as HTL

Simulation of various inorganic metal HTLs

In simulations, the same parameters as in Table 1 are used to analyze the impact of different HTLs (Spiro-OMeTAD, NiO, Cu2O, and CuO) on PCE across a variety of solar cell-based devices. Figure 3 revealed that Spiro-OMeTAD has a higher η (10.19%) than Cu2O, CuO, and NiO (9.96%, 8.79%, and 8.66%, respectively). Using Spiro-OMeTAD as the HTL increased the η in perovskite solar cells as demonstrated by [33]. As well as, [34], also stated that the stable Spiro-OMeTAD produces a typical HTL as the top layer of a perovskite solar cell.

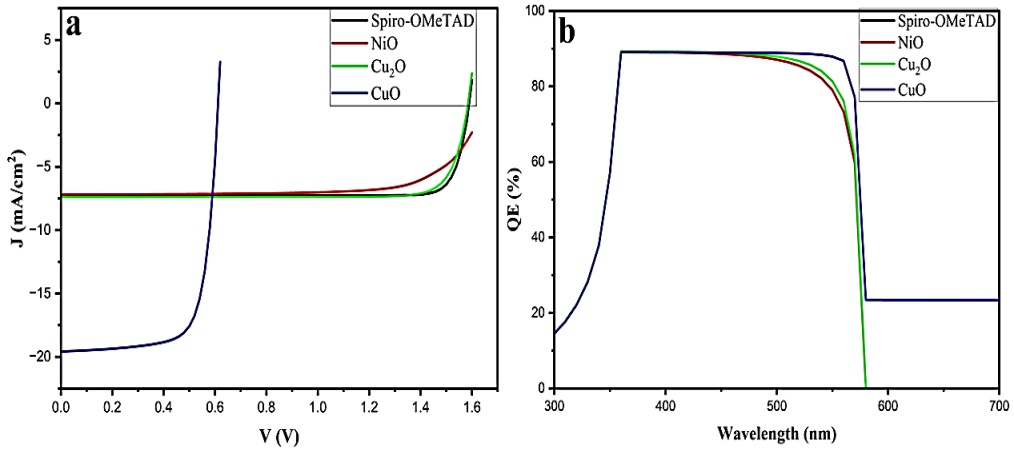

Fig. 3: (a): illuminated J-V and, (b): QE of different-configuration using of various HTL and SnO_2 as ETL.

SnO_2 and Spiro-OMeTAD serve as the ETL and HTL, respectively, in the n-i-p configuration. They are (35 nm) thick for SnO_2, (350 nm) thick for Spiro-OMeTAD, and (900 nm) thick for methyl ammonium tin chloride ($CH_3NH_3SnCl_3$). Under AM (1.5 G), the output parameters are shown in Table 3.

Table 3: Effects of HTL on the output parameters of the n-i-p PSC

Cell parameters	Spiro-OMeTAD	NiO	Cu_2O	CuO
V_{oc} (V)	1.58	1.66	1.58	0.61
J_{sc} (mA/cm^2)	7.28	7.19	7.39	19.58
FF (%)	88.00	72.26	85.02	73.34
η (%)	10.19	8.66	9.96	8.79

Effect of total Defect Density of Tin oxide

The N_t influences the performance of photovoltaic solar cells because defects accelerate the recombination of photo-generated carriers in perovskite solar cells, leading to increased recombination. We have investigated the impact of the N_t of SnO_2 on the performance of perovskite solar cells by varying the number from (10^{13} cm^{-3}) to (10^{20} cm^{-3}). Figure 4 presents the simulation results. The rise in total defect density to values higher than (10^{15} cm^{-3}) for SnO_2 leads to a reduction

in PV parameters. The result agreed with [35], which revealed that the presence of recombination centers resulting from the defect reduces the device's open-circuit voltage (V_{oc}) by reducing shunt resistance. This recombination reduces the quasi-Fermi level splitting in the device, which directly lowers V_{oc}.

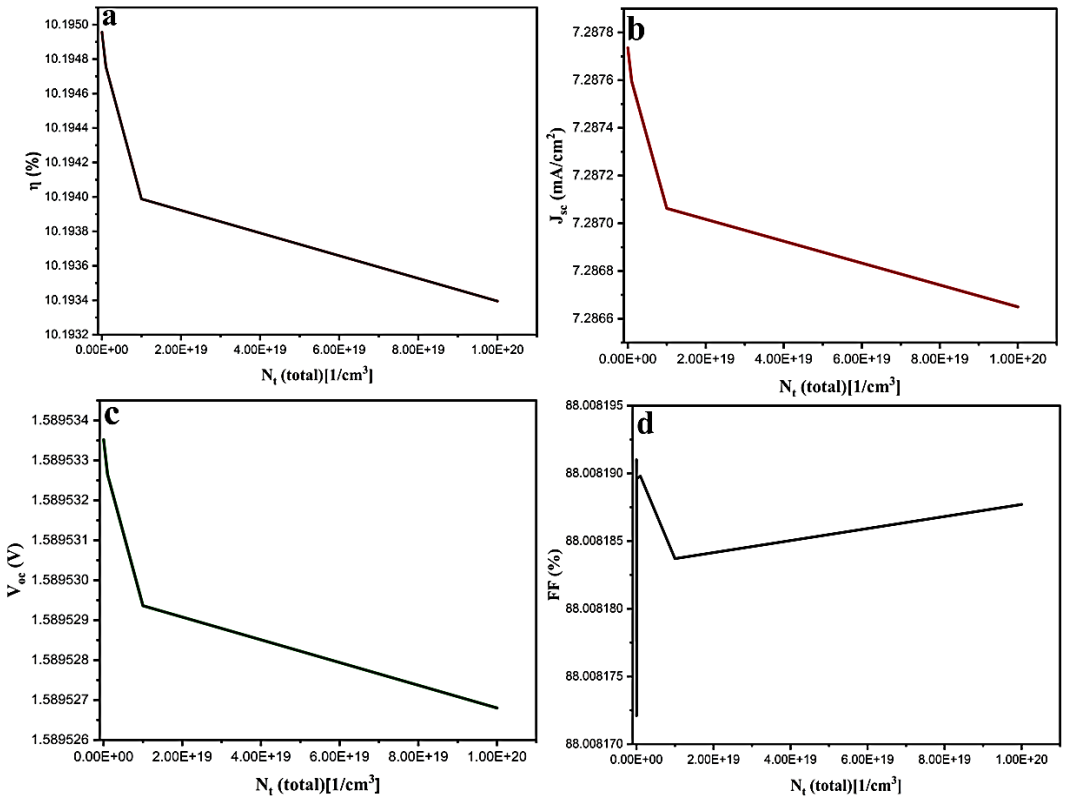

Fig. 4: Varying (a) η, (b) J_{sc}, (c) V_{oc} and (d) FF with total defect density of tine oxide

Effect of total Defect Density of absorbers layer

Figure 5 shows a numerical analysis of suggested Sn-based perovskite solar cell response to variations in total defect density of absorber layer, which directly influence the perovskite solar cell efficiency. The total defect density (N_t) of the absorbers layer varies from (10^9 cm^{-3}) to (10^{13} cm^{-3}). The output parameters decrease from η (13.68 % to 10.19 %), V_{oc} (1.6 V to 1.58 V), J_{sc} (9.65 mA/cm^2 to 7.28 mA/cm^2) and FF (88.38 % to 88 %) as the defect density exceeds (10^9 cm^{-3}) leading to an increase in recombination rates. Furthermore, the effectiveness decreases as the quantity of total defect density increases, mostly lead to a decrease in the distance that the charge-carriers travel [36,37].

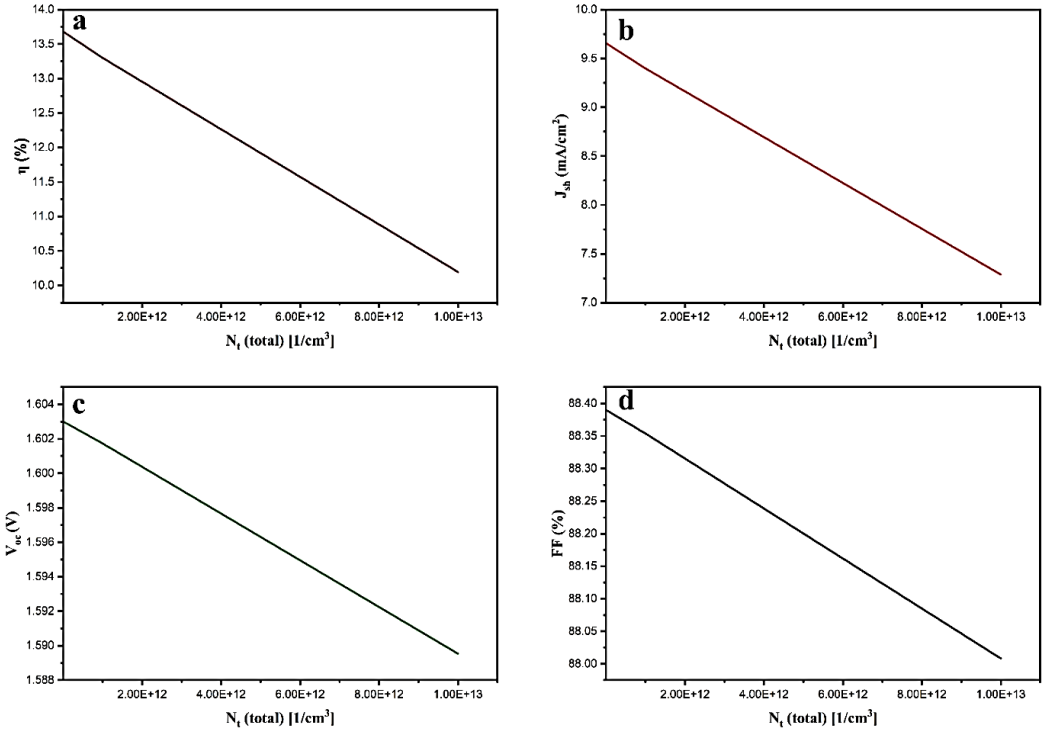

Fig. 5: Varying (a) η, (b) J_{sc}, (c) V_{oc} and (d) FF with N_t in absorber layer

Effect of total Defect Density on HTLs

Defects in solar cells are undesirable because they adversely affect both efficiency and stability. The total N_t of the Spiro-OMeTAD is within the range of (10^{10} cm^{-3}) to (10^{19} cm^{-3}), as suggested. The results depicted in Figure 6 demonstrate an increase in defect density for Spiro-OMeTAD, leading to slightly decreasing output PV parameters as total N_t were larger than (10^{14} cm^{-3}). While, the performance of solar cells does decline as the defect density increases, the overall impact on the results was not substantial. A higher defect density leads to an increased recombination rate, thereby reducing carrier lifetime. The performance of solar cells is highly sensitive to defect density. While low defect levels have minimal impact, increasing defect density exponentially accelerates recombination and efficiency loss. Optimizing material quality and defect management is key to sustaining high-performance solar cells.

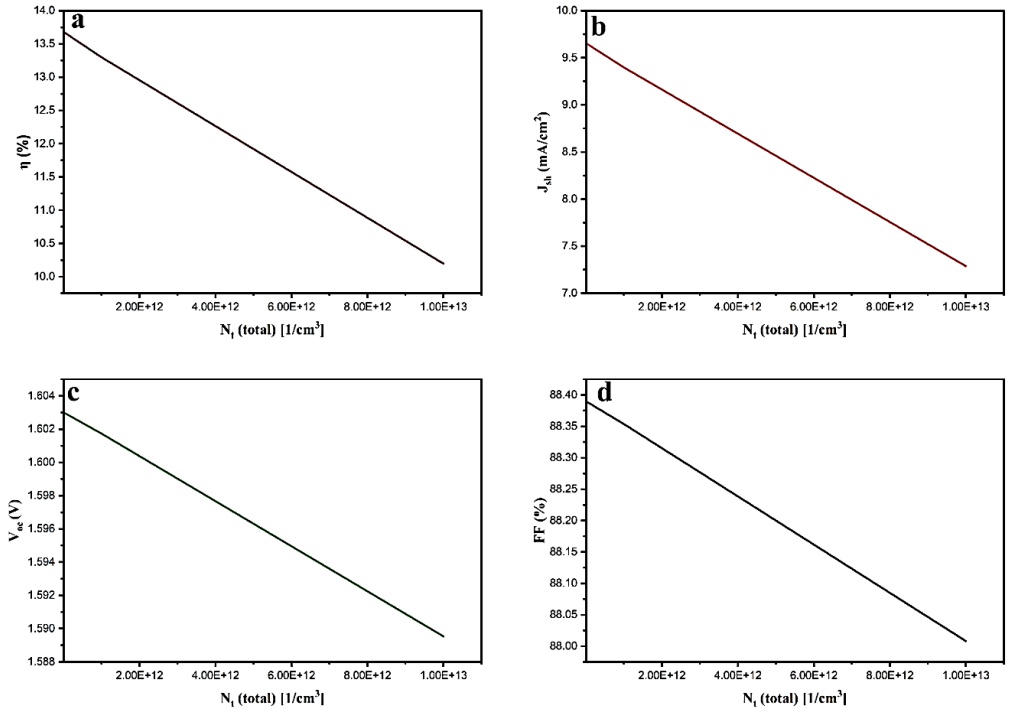

Fig. 6: Varying (a) η, (b) J_{sc}, (c) V_{oc} and (d) FF with total defect density of HTL.

Figure 7 illuminates J-V characteristics of the final model of an optimized cell which consist an ETL, absorbers, and HTL layers. Each of the layers had a total defect density of (10^{14} cm^{-3}, 10^{7} cm^{-3}, and 10^{6} cm^{-3}), respectively. The efficiency was (13.68 %) as illustrated in Table 4. As the overall defect density of the absorber layer increases, Jsc decreases. This is because an increased defect density results in a higher recombination rate, which in turn affects carrier lifetimes. [38,39]. Shockley-Read Hall (SRH) recombination occurs due to defects in the energy band gap, leading to a decrease in efficiency [40].

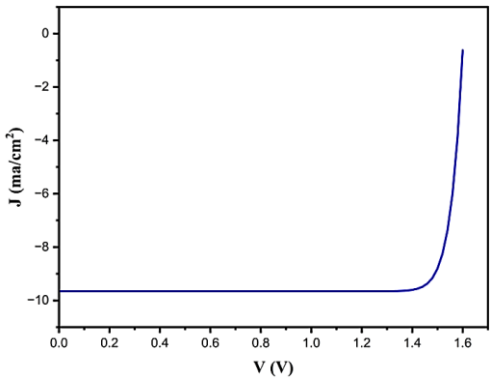

Fig. 7: Illuminated J-V characteristics of optimized (FTO/glass/ SnO_2/ $CH_3NH_3SnI_3$/Spiro OMe-TAD/ Au) solar cell

Table 4: Final device performance (FTO/glass/ SnO_2/ $CH_3NH_3SnCl_3$/Spiro OMe-TAD/Au) on the basis of optimized parameters

V_{oc}	1.60 (Volt)
J_{sc}	9.65 mA/cm^2
FF	88.34 %
H	13.68 %

CONCLUSION

This study employed several n-i-p configurations to identify more appropriate ETL and HTL for the lead-free absorbent layer ($CH_3NH_3SnCl_3$). The investigation of IGZO, SnO_2, TiO_2, and ZnO as ETL -layers and Spiro-OMeTAD, NiO, Cu_2O, and CuO as HTL and tin oxide revealed greater η and is thought to be suitable for ETLs and a good HTL is Spiro-OMeTAD. The results showed that the (SnO_2/$CH_3NH_3SnCl_3$/Spiro-OMeTAD/gold) structure of the perovskite solar cell is the most efficient configuration, with output parameters of (Voc = 1.58 V, Jsc = 7.28 mA/cm2, FF = 88.00%, and η = 10.19%). Additionally, the total defect densities of SnO_2, $CH_3NH_3SnCl_3$, and Spiro-OMeTAD are optimized, and the results suggest that SnO_2 (10^{15} cm^{-3}), perovskite layer (10^{9} cm^{-}

^{3}), and Spiro-OMeTAD layer (10^{14} cm^{-3}) to attain high performance of perovskite solar cells: (V_{oc}=1.6 V, J_{sc}=9.65 mA/cm^2, FF=88.34 %, and η=13.68 %). The absorber layer is more affected by the N_t than the two other layers (SnO_2 and Spiro-OMeTAD). The simulation results used to create environmentally friendly, high-efficiency perovskite solar cells.

Conflict of interests: The authors declare that they have no conflicts of interest

Sources of funding: The authors state they are self-funded

Author contributions: The authors contributed to the conception and design, acquisition of data, or analysis and interpretation of data.

REFERENCES

1. Lye YE, Chan KY, Ng ZN. A review on the progress, challenges, and performances of tin-based perovskite solar cells. Nanomaterials. 2023 Feb 1;13(3):585. https://doi.org/10.3390/nano13030585.

2. Dris K, Benhaliliba M, Ayeshamariam A, Roy A, Kaviyarasu K. Improving the perovskite solar cell by insertion of methyl ammonium tin oxide and cesium tin chloride as absorber layers: scaps 1d study based on experimental studies. Journal of Optics. 2024:1-23. https://ui.adsabs.harvard.edu/link_gateway/2024JOpt..tmp..385D/doi:10.1007/s12596-024-01996-7.

3. Moyez SA, Roy S. Thermal engineering of lead-free nanostructured $CH_3NH_3SnCl_3$ perovskite material for thin-film solar cell. Journal of Nanoparticle Research. 2018;20:1-13. https://ui.adsabs.harvard.edu/link_gateway/2018JNR....20....5M/doi:10.1007/s11051-017-4108-z

4. Deng P, Dai W, Gou Y, Zhang W, Xiao Z, He S, Xie X, Zhang K, Li J, Wang X, Lin L. Improving Thermal Stability of High-Efficiency Methylammonium-Free Perovskite Solar Cells via Chloride Additive Engineering. ACS Applied Materials & Interfaces. 2024 May 21. https://doi.org/10.1021/acsami.4c01335.

5. Chen P, Pan W, Zhu S, Cao F, Tong A, He R, Lan Z, Sun W, Wu J. Buried modification with tetramethylammonium chloride to enhance the performance of perovskite solar cells with nip structure. Chemical Engineering Journal. 2023 Jul 15;468:143652. https://ui.adsabs.harvard.edu/link_gateway/2023ChEnJ.46843652C/doi:10.1016/j.cej.2023.143652.

6. Liu J, Chen X, Chen K, Tian W, Sheng Y, She B, Jiang Y, Zhang D, Liu Y, Qi J, Chen K. Electron injection and defect passivation for high-efficiency mesoporous perovskite solar cells. Science. 2024 Mar 15;383(6688):1198-204. https://doi.org/10.1126/science.adk9089

7. Weerasinghe HC, Macadam N, Kim JE, Sutherland LJ, Angmo D, Ng LW, Scully AD, Glenn F, Chantler R, Chang NL, Dehghanimadvar M. The first demonstration of entirely roll-to-roll fabricated perovskite solar cell modules under ambient room conditions. Nature Communications. 2024 Mar 12;15(1):1656. https://doi.org/10.1038/s41467-024-46016-1.

8. Gopinathan N, Basha SS, Vasimalai N, Mundari NA, Shajahan A, Parveen JS, Enayathali SS. Composition-Driven Structural, Optical, Thermal and Electrochemical Properties of Hybrid Perovskite-Structured Methylammonium-Tin-Chloride. Journal of Electronic Materials. 2024 Jan;53(1):94-105. https://ui.adsabs.harvard.edu/link_gateway/2024JEMat..53...94G/doi:10.1007/s11664-023-10777-0.

9. Sahoo D, Karan AK, Manik NB. Study on the effect of temperature on electrical parameters of lead free methylammonium tin halide based Perovskite Schottky Devices. International Journal of Innovative Research in Physics. 2022;4(1):6-16. http://dx.doi.org/10.15864/ijiip.4102

10. Singh PK, Singh R, Singh V, Bhattacharya B, Khan ZH. New class of lead free perovskite material for low-cost solar cell application. Materials Research Bulletin. 2018;97:572-7. https://doi.org/10.1016/j.materresbull.2017.09.054

11. Thankappan A. Numerical simulation of solar cell performance with copper-based layered

perovskite using SCAPS 1D software. Model Simul Mater Sci Eng. 2024;32:015010. http://dx.doi.org/10.1088/1361-651X/ad104e

12. Arif F, Aamir M, Shuja A, Shahiduzzaman M, Akhtar J. Simulation and numerical modeling of high performance $CH_3NH_3SnI_3$ solar cell with cadmium sulfide as electron transport layer by SCAPS-1D. Results in Optics. 2024;14:100595. https://doi.org/10.1016/j.rio.2023.100595

13. Salem MS, Shaker A, Zekry A, Abouelatta M, Alanazi A, Alshammari MT, Gontand C. Analysis of hybrid hetero-homo junction lead-free perovskite solar cells by SCAPS simulator. Energies. 2021 Sep 12;14(18):5741. https://doi.org/10.3390/en14185741.

14. Rehman A, Munir T, Afzal S, Saleem M, Ikhioya IL. Enhanced Solar Cell Efficiency with Tin-Based Lead-Free Material ($FASnI_3$) through SCAPS-1D Modeling. Eurasian Journal of Science and Technology. 2024;4(3). https://doi.org/10.48309/ejst.2024.429200.1118

15. Slami A, Bouchaour M, Merad L. Comparative study of modelling of Perovskite solar cell with different HTM layers. Int J Mater. 2020;7(July). http://dx.doi.org/10.46300/91018.2020.7.1

16. Shamna M, Nithya K, Sudheer K. Simulation and optimization of $CH_3NH_3SnI_3$ based inverted perovskite solar cell with NiO as Hole transport material. Materials Today: Proceedings. 2020;33:1246-51. http://dx.doi.org/10.1016/j.matpr.2020.03.488

17. Mandadapu U, Vedanayakam SV, Thyagarajan K, Babu B. Optimisation of high efficiency tin halide perovskite solar cells using SCAPS-1D. International Journal of Simulation and Process Modelling. 2018;13(3):221-7. http://dx.doi.org/10.1504/IJSPM.2018.093097

18. Sunny A, Rahman S, Khatun MM, Ahmed SRA. Numerical study of high performance HTL-free $CH_3NH_3SnI_3$-based perovskite solar cell by SCAPS-1D. AIP Advances. 2021;11(6):065102. https://doi.org/10.1063/5.0049646.

19. Patel PK. Device simulation of highly efficient eco-friendly $CH_3NH_3SnI_3$ perovskite solar cell. Scientific Reports. 2021;11(1):1-11. https://doi.org/10.1038/s41598-021-82817-w

20. Azri F, Meftah A, Sengouga N, Meftah A. Electron and hole transport layers optimization by numerical simulation of a perovskite solar cell. Solar energy. 2019;181:372-8. http://dx.doi.org/10.1016/j.solener.2019.02.017.

21. Madan J, Pandey R, Sharma R. Device simulation of 17.3% efficient lead-free all-perovskite tandem solar cell. Solar energy. 2020;197:212-21. http://dx.doi.org/10.1016/j.solener.2020.01.006

22. De Los Santos IM, Cortina-Marrero HJ, Ruíz-Sánchez MA, Hechavarría-Difur L, Sánchez-Rodríguez FJ, Courel M, Hu H. Optimization of $CH_3NH_3PbI_3$ perovskite solar cells: A theoretical and experimental study. Solar Energy. 2020 Mar 15;199:198-205. https://doi.org/10.1016/j.solener.2020.02.026

23. Hima A, Lakhdar N, Saadoune A. Effect of Electron Transporting Layer on Power Con-version Efficiency of Perockite-based Splar Cell: Comparative Study. Журнал нано-та електронної фізики. 2019(11,№ 1):01026-1-5. http://dx.doi.org/10.21272/jnep.11(1).01026

24. Aseena S, Abraham N, Babu VS. Optimization of layer thickness of ZnO based perovskite solar cells using SCAPS 1D. Materials Today: Proceedings. 2021;43:3432-7. https://doi.org/10.1016/j.matpr.2020.09.077

25. Casas G, Cappelletti MÁ, Cedola AP, Soucase BM, y Blancá EP. Analysis of the power conversion efficiency of perovskite solar cells with different materials as Hole-Transport Layer by numerical simulations. Superlattices and Microstructures. 2017;107:136-43. http://dx.doi.org/10.1016/j.spmi.2017.04.007

26. Shoab M, Aslam Z, Zulfequar M, Khan F. Numerical interface optimization of lead-free perovskite solar cells ($CH_3NH_3SnI_3$) for 30% photo-conversion efficiency using SCAPS-1D. Next Materials. 2024;4:100200. https://doi.org/10.1016/j.nxmate.2024.100200

27. Krishnan A, Subash T. Simulation of NiOx Based Solar Cells Using SCAPS Software. NanoWorld J. 2023;9(S5):S143-S8. https://doi.org/10.17756/nwj.2023-s5-028

28. Najim AH, Saleh AN. Study effect of window and BSF layers on the properties of the CZTS/CZTSe solar cell by SCAPS–1D. Tikrit Journal of Pure Science. 2019;24(3):77-83. https://doi.org/10.25130/tjps.v24i3.372

29. Razooqi MA, Majeed ZN. The Effect of Copper Doping on Some Structural and Electrical Properties of Titanium Dioxide Nanofilms. Tikrit Journal of Pure Science. 2023;28(6):51-7. https://doi.org/10.25130/tjps.v28i6.1377

30. Moiz SA, editor Optimization of Hole and Electron Transport Layer for Highly Efficient Lead-Free Cs_2TiBr_6-Based Perovskite Solar Cell. Photonics; 2021: MDPI. https://doi.org/10.3390/photonics9010023

31. Bhavsar K, Lapsiwala P. Numerical simulation of perovskite solar cell with different material as electron transport layer using SCAPS-1D software. Semiconductor Physics, Quantum Electronics & Optoelectronics. 2021;24(3):341-7. https://doi.org/10.15407/spqeo24.03.341

32. Hongsith K, Yarangsi V, Sucharitakul S, Phadungdhitidhada S, Ngamjarurojana A, Choopun S. A Multi-Electron Transporting Layer for Efficient Perovskite Solar Cells. Coatings. 2021;11(9):1020. https://doi.org/10.3390/coatings11091020.

33. Okada Y, Suzuki A, Yamasaki Y, Oku T. Fabrication and characterization of perovskite based solar cells using phthalocyanine and naphthalocyanine as hole-transporting layer. AIP Conference Proceedings; 2017: AIP Publishing LLC. https://doi.org/10.1063/1.4974797.

34. Mishra K, Chauhan R, Mishra R, Srivastava V. Performance optimization of lead-free inorganic perovskite solar cell using SCAPS-1D. Journal of Optics. 2024;53(3):2668-78. http://dx.doi.org/10.1007/s12596-023-01466-6

35. Moinuddin RM, Hasan M, Rahaman M, Islam KS. Numerical optimization and efficiency analysis of Sn-based perovskite-on-silicon tandem solar cells with various TCO materials using SCAPS-1D simulation. AIP Advances. 2024;14(8). http://dx.doi.org/10.1063/5.0217477

36. Biswas SK, Sumon MS, Sarker K, Orthe MF, Ahmed MM. A Numerical Approach to Analysis of an Environment-Friendly Sn-Based Perovskite Solar Cell with SnO_2 Buffer Layer Using SCAPS-1D. Advances in Materials Science and Engineering. 2023;2023(1):4154962. http://dx.doi.org/10.1155/2023/4154962.

37. Vaish S, Dixit SK. Study the effect of total defect density variation in absorbing layer on the power conversion efficiency of lead halide perovskite solar cell using SCAPS-1D simulation tool. Materials Today: Proceedings. 2023;91:17-20. https://doi.org/10.1016/j.matpr.2023.05.374.

38. Jamal MS, Shahahmadi SA, Wadi MA, Chelvanathan P, Asim N, Misran H, Hossain MI, Amin N, Sopian K, Akhtaruzzaman M. Effect of defect density and energy level mismatch on the performance of perovskite solar cells by numerical simulation. Optik. 2019 Apr 1;182:1204-10. https://doi.org/10.1016/j.ijleo.2018.12.163

39. Ganem HT, Saleh AN. The effect of band offsets of absorption layer on CNTS/ZnS/ZnO solar cell by SCAPS-1D. Tikrit Journal of Pure Science. 2020 Dec 23;25(6):79-87. **https://doi.org/10.25130/tjps.v25i6.316**

40. Kothandapani Z, Islam M, Reza Y, Hasana A, Amin N. Optimization of Cu_2O and CuSCN as HTL of planar perovskite solar cells via numerical simulation. Journal of Ovonic Research Vol. 2020;16(6):369-77. http://dx.doi.org/10.15251/JOR.2020.166.369.